Journal of Current Science and Technology, January-April 2022 Vol. 12 No. 1, 43-51
ISSN 26300656 (Online)

Cite this article: Padmasini, N., Aarthi, J., Deepika, U., & Deepshikhaa, R. (2022, January). Iridology based diagnosis of kidney abnormalities due to diabetes mellitus. *Journal of Current Science and Technology*, *12*(1), 43-51. DOI:

Journal of Current Science and Technology
Journal homepage: https://jcst.rsu.ac.th

Iridology based diagnosis of kidney abnormalities due to diabetes mellitus

N. Padmasini*, J. Aarthi, U. Deepika, and R. Deepshikhaa

Department of Biomedical Engineering, Rajalakshmi Engineering College, Chennai, India 602 105

*Corresponding author; E-mail: padmasini.n@rajalakshmi.edu.in

Received 8 July 2021; Revised 5 September 2021; Accepted 10 September 2021;
Published online 25 January 2022

Abstract

Iridology is a very useful technique to diagnose the abnormalities in various parts of our human body. The human iris is connected to all parts of the body through nerve strands. Iridologists see the eyes as windows into the body's state of health through iris images. Iridologists claim they can use the iridology charts to distinguish between healthy organs and those that are overactive, inflamed, or distressed through the change in pigmentation or due to lacunae formation in the various iris regions. Asthe diabetic population is increasing day by day, it is crucial to detect early changes in the kidneys due toType 1 or Type 2 diabetes, in order to avoid kidney failure. This work aims to diagnose the presence of any abnormality in the kidney due to diabetes mellitus using iris images as well as iridology charts and hence, automatically categorizing normal and abnormal cases using the Random Forest Classification algorithm. Through this algorithm 83.33 percent accuracy is achieved. As a pilot study twenty four normal and abnormal images were taken and analyzed. However, more images are to be analysed to claim iridology as a tool for diagnosing kidney ailments.

Keywords**:** *GLCM; histogram; iridology; iriscope, iris chart; kidney; Random Forest Classification.*

1. Introduction

The iris is a thin, circular structure in the eye, responsible for controlling the diameter and size of the pupil and thus the amount of light reaching the retina. Eye color is defined by that of the iris. In optical terms, the pupil is the eye's aperture, while the iris is the diaphragm (Chaskar & Sutaone, 2012).

The iris is divided into two major regions: (a) The pupillary zone, which is the inner region whose edge forms the boundary of the pupil and (b) The ciliary zone is the rest of the iris that extends to its origin at the ciliary body. From anterior (front) to posterior (back), the layers of the iris are : Anterior limiting layer, Stroma of iris, Iris sphincter muscle, Iris dilator muscle (myoepithelium), Anterior pigment epithelium, Posterior pigment epithelium (Othman, Zuraini, and Anton Satria Prabuwono,2010)

1.1 Iris chart and its significance

A typical iris chart usually divides the iris into approximately 90 zones, each corresponding to a different part of the human body. Iridologists believe that the details reflected by the iris are generally the changes in the tissues of the specific body organelle. Iridology is one way of analyzing health based on the iris (Asuntha, Siddartha, Udhaykumar, & Srinivasan, 2019).

The iris chart shown in Figure 1 and Figure

2 are redrawn from the original chart of Jensen, 2012, which shows the kidney region is between 200 to 210 degrees if we consider the chart as a 360 degree image (Prayitno, Wibawa, & Purnomo, 2016). Except for the kidney region, all other regions are masked and the kidney region alone is cropped. The cropped region is processed and analyzed. As the texture of the region is varied in kidney abnormalities, the features are extracted from texture analysis (Bansal, Agarwal, & Sharma, 2015). In order to obtain good accuracy, identification of best features is very crucial (Hiremath, Vajrala, Balakrishnan, Yeshwanth, & Jayantha, 2018). The extracted features are analysed by comparing the results of normal and kidney disease affected patients (Hussein, Hassan, & Granat, 2013). In the work by Amerifar, Targhi, and Dehshibi (2015) 82 percent accuracy was obtained in diagnosing kidney disease from iris images. Jogi and Sharma (2014) have used a linear normalization technique for localizing the region of interest. For the detection of diabetes from a total of 358 iris images an accuracy of 89.63 percent is achieved by Samant and Agarwal (2018). A comparative study on Iris manifestations between COVID-19 severe Cases and non-COVID individuals was performed by Ayda et al. (2021).

In this present work we mainly focus on the kidney region. Iris images are obtained from both normal as well as kidney abnormality affected patients. The subject's physiological parameters are also considered. The region of interest, i.e the kidney portion, alone is segmented and the features from this region are extracted and classified automatically as normal and abnormal using the Random Forest classifier.

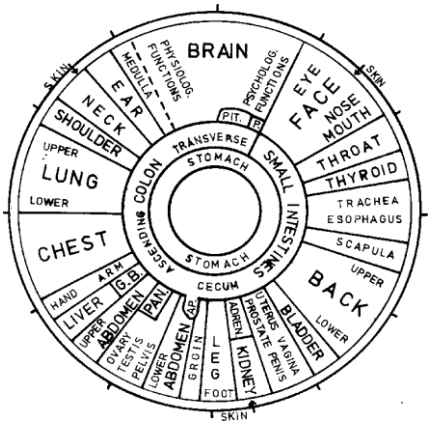

Figure 1 Right iris chart

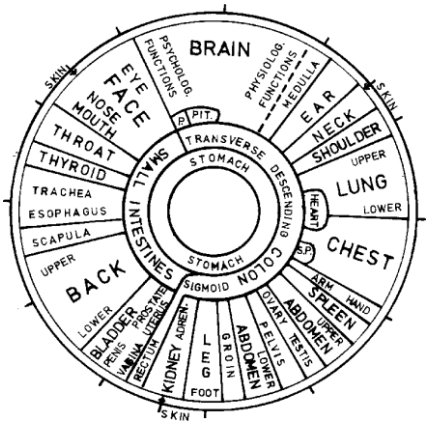

Figure 2 Left iris chart

2. Objective

The objective of the work is to develop a noninvasive system for the detection of kidney abnormalities due to diabetes mellitus. We also aimed to evaluate the system using the best machine learning algorithm.

3. Materials and methods

In this work for the capture of iris images, a digital iriscope is used as shown in Figure 3. The model used is MM-MIRS-9130U.

The specification of this USB digital iriscope is as follows. The viewable magnification ratio is 10 to 20X. The resolution of the image sensor is 1.30 megapixels (1/4 inch). The video capture resolution is 1,280 x 1,024, 640 x 480, 320 x 240 pixels and the still image capture resolution is 1,280 x 1,024 pixels

Figure 3 Digital iriscope

3.1 Step by step procedure for capture of iris image

Step 1:

The subject is made to sit upright and his/her iris images from both right and left eye are captured. A typical iris image captured by this iriscope is shown in Figure 4

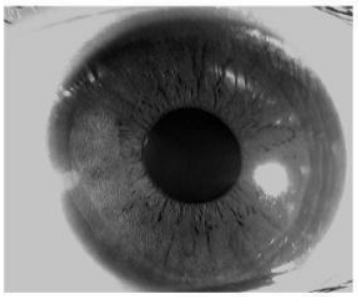

Figure 4 Typical iris image

Step 2:

Figure 5A shows a typical iris image, with kidney and pancreas regions marked. The transparent iris chart of the right eye, shown in Figure 5B, is initially created using photo shop, from the standard Iris chart coined by Bensen. The transparent chart is carefully placed over the acquired image so that it exactly coincides as shown in Figure 5C and the Region of Interest (ROI) is cropped carefully. Following this the ROI is converted into a grayscale image.

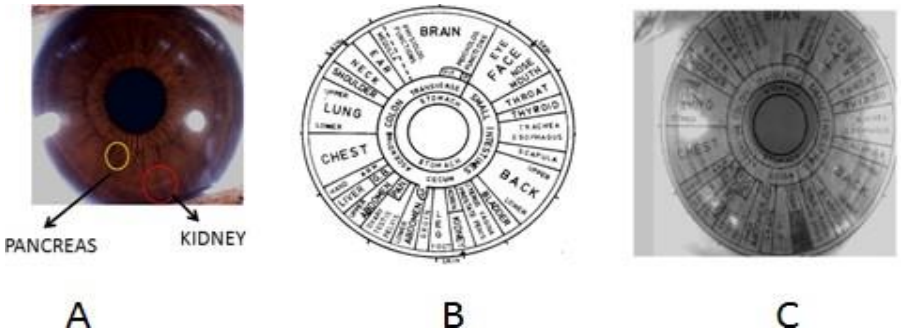

Figure 5. Overlapped transparency chart over the captured image JCST

Step 3:

Now the converted image is pre-processed by histogram equalisation. This is done to improve the quality of the image and also to increase the contrast of the image (Shampine & Reichelt, 1997).

Step 4:

Except for the Region of Interest (ROI), the other portions are masked by using Free Hand Masking technique. Masking is done to conceal the unwanted portions of the image as shown in Figure 6.

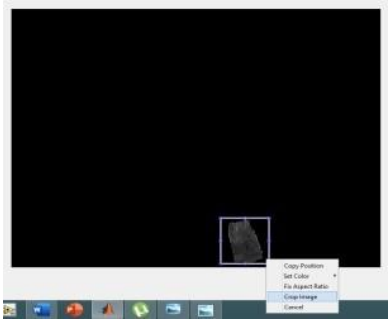

Figure 6 Cropping the ROI and masking the rest of the portion

Step 5:

After masking the Region of Interest is segmented. Segmentation is done by cropping specific regions fromthe image as shown in Figure 7. Cropping is also done to remove the unwanted regions from the image.

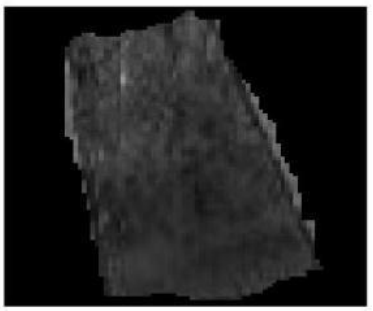

Figure 7. Segmented region of interest

Step 6:

Required features are extracted from the segmented region using GLCM (Gray Level Co-occurrence Matrix) method (Asuntha et al., 2019). GLCM is a way of extracting second order statistical texture features. From the GLCM matrix the features such as Contrast, Homogeneity,

Energy, Entropy and Correlation are extracted. These features are given as input to the classifier unit which is explained in the following step.

Step 7:

The final step is classification. For this we use the Random Forest Classification method. Many machine learning techniques can be used for classification. Amongst all, Random Forest Classification is proved to be the best method which yields good accuracy (Padmasini, Umamaheswari, Kalpana, & Sikkandar, 2020). It creates a set of decision trees from a randomly selected subset of the training set and hence the sensitivity as well as precision is also good.

4 Results and discussion

In this work 24 normal subjects and 24 subjects with kidney abnormalities are taken into account. The GLCM features are extracted from the iris images of all the 48 subjects as shown in Table 1. These parameters are given as input to the Random Forest classifier. These features are trained with the values as 0 for normal cases and 1 for kidney abnormality cases as shown in Table 1.

Table 1 Extraction of features from the segmented portion

Subject	Correlation	Homogeniety	Energy	Contrast	Entropy	Prediction
1	0.6982	0.9196	0.4811	0.1699	5.8927	1
2	0.807	0.9196	0.4811	0.1699	5.8927	1
3	0.6982	0.9258	0.3155	0.1931	4.9381	1
4	0.8086	0.9275	0.3139	0.1672	4.1443	1
5	0.8369	0.9381	0.3403	0.1941	3.7221	1
6	0.8354	0.9418	0.3751	0.1627	4.9373	1
7	0.8328	0.9423	0.3926	0.1635	3.5399	1
8	0.8294	0.9362	0.3889	0.1746	3.5385	1
9	0.8176	0.939	0.3385	0.1984	3.7214	1
10	0.7989	0.9318	0.365	0.1711	4.1457	1
11	0.7732	0.9192	0.3219	0.2327	4.1457	1
12	0.6354	0.9087	0.3572	0.1843	4.3636	1
13	0.4810	0.8798	0.3616	0.2427	5.2225	1
14	0.6394	0.9095	0.3583	0.1826	4.3639	1
15	0.6956	0.9305	0.4332	0.1398	3.663	1
16	0.7273	0.9432	0.4924	0.1143	3.2382	1
17	0.7384	0.9475	0.5146	0.1055	3.0794	1
18	0.7477	0.9497	0.5203	0.1012	3.0792	1
19	0.7476	0.9477	0.5008	0.1053	3.2396	1
20	0.7527	0.9439	0.4545	0.1131	3.6611	1
21	0.7257	0.9315	0.3902	0.1382	4.3636	1
22	0.6226	0.9122	0.3982	0.1770	5.2225	1
23	0.7284	0.9321	0.3907	0.1371	4.3639	1
24	0.7497	0.9431	0.4535	0.1145	3.6630	1
25	0.6645	0.9230	0.5088	0.1619	5.7859	0
26	0.8157	0.923	0.5088	0.1619	5.7859	0
27	0.6645	0.9313	0.3264	0.1774	4.8000	0
28	0.8085	0.9307	0.3261	0.1517	4.0555	0

Subject	Correlation	Homogeniety	Energy	Contrast	Entropy	Prediction
29	0.8389	0.9416	0.3506	0.1709	3.6366	0
30	0.8400	0.9452	0.3836	0.1458	4.801	0
31	0.8348	0.9447	0.4011	0.1475	3.4494	0
32	0.8337	0.94	0.3981	0.1546	3.4487	0
33	0.8246	0.9423	0.3482	0.1761	3.6382	0
34	0.8068	0.9351	0.3732	0.1559	4.0586	0
35	0.7804	0.9231	0.3301	0.2076	4.0586	0
36	0.8345	0.9002	0.295	0.2697	4.8010	0
37	0.7087	0.9429	0.4599	0.2843	5.7859	0
38	0.9030	0.9281	0.2753	0.1535	6.4573	0
39	0.8935	0.9276	0.2067	0.2917	5.3865	0
40	0.9073	0.9371	0.262	0.2603	4.5250	0
41	0.9116	0.9409	0.3101	0.2393	4.0600	0
42	0.9124	0.9432	0.3371	0.2304	3.8284	0
43	0.9120	0.9426	0.3356	0.2320	3.8283	0
44	0.9082	0.9374	0.3046	0.2477	4.06	0
45	0.8990	0.9249	0.2501	0.2838	4.5238	0
46	0.8753	0.9053	0.1881	0.3408	5.3856	0
47	0.8763	0.9111	0.2545	0.2045	6.4573	0
48	0.8763	0.9111	0.2545	0.2045	6.4573	0

All the above features are trained and validated using different tree models in the Random Forest Classifier.The accuracy of all the three tree models such as fine, medium and coarse trees resulted in an accuracy of 83.3%, as shown in Figure 8.

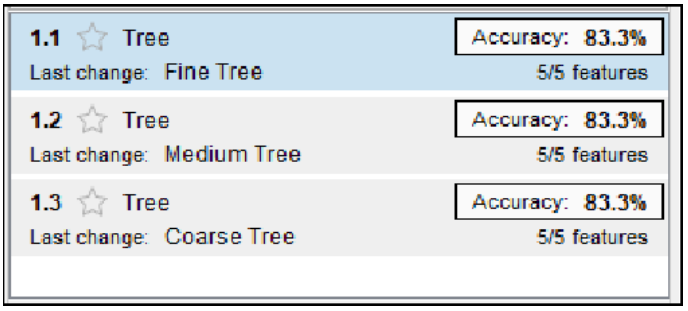

Figure 8 Accuracy of tree models

The confusion matrix of the classifier is shown in Figure 9.

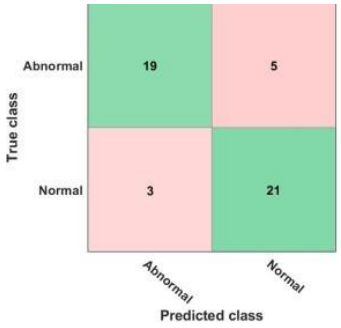

Figure 9 Confusion matrix of Random Forest Classifier

From the confusion matrix in Figure 9, the top left corner first element indicates that among 24 abnormal images 19 images are correctly identified and the rest of the 5 images are wrongly identified as normal.

It gives the correctly predicted classes. Among 24 normal classes 21 classes are predicted to be correct and among 24 abnormal images with kidney ailments, 19 images were correctly identified. True positive and false negative rate is shown in Figure 10. Positive predictive value is the probability that indicates how many subjects have been identified truly as they are having the disease. It is similar to sensitivity

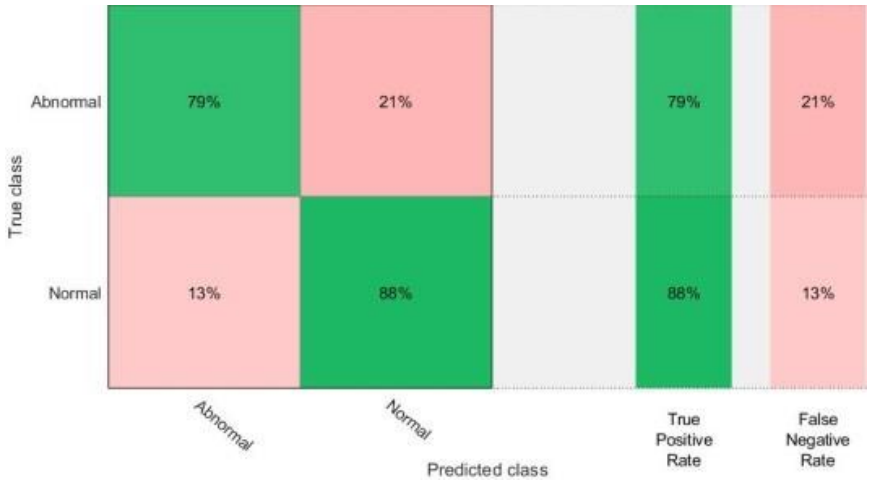

Figure 10. True positive rate

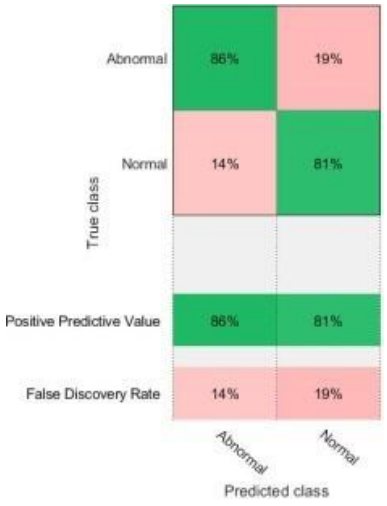

Figure 11 Positive predictive value

The positive predictive values (PPV) are shown in Figure 11 and the Receiver Operating Characteristic (ROC) curve with True positive Vs false positive rates is shown in Figure 12. The parallel coordinates plot of this model is shown in Figure 13. Parallel coordinates plot is used in data analysis where many quantitative variables could be compared together by seeing the patterns involved and hence the relationship between them could be analysed.

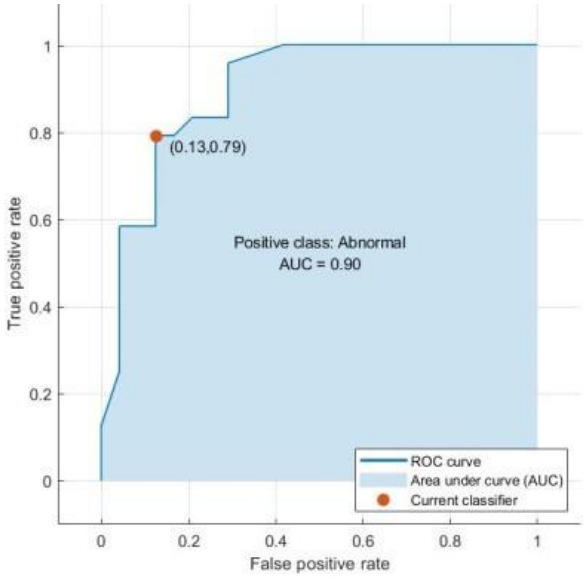

Figure 12 ROC curve

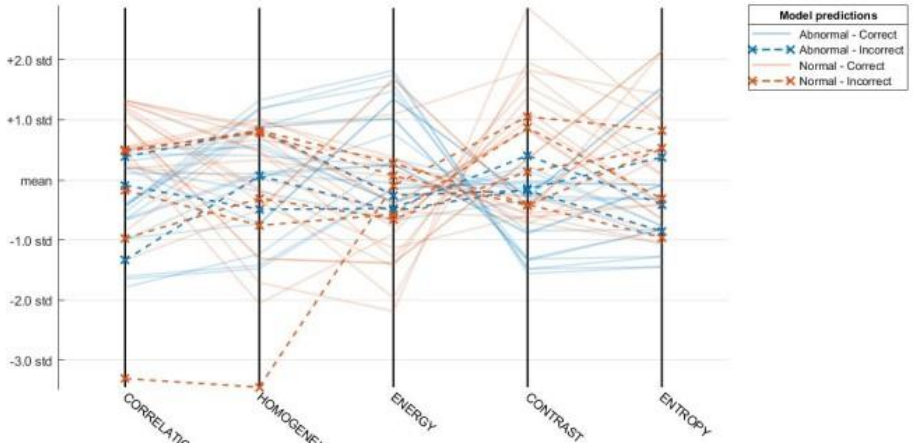

Figure 13 Parallel coordinates plot

5. Conclusion

This paper emphasizes a replacement framework for the detection of kidney abnormalities in diabetic patients from the Iris images. Twenty four normal as well as twenty four abnormal images with kidney abnormalities are considered. The kidney region in the iris image (200-210 degrees) is segmented by making use of a transparency iridology chart. The region of interest is analyzed by extracting the textural features. The features are given as input to the Random forest classifier and the system is trained and validated. The validation accuracy of the system is observed to be good. This alternative method of noninvasive diagnosis will be a most helpful promising tool in early stage diagnosis of kidney disease due to diabetes. During this pandemic situation we were able to collect only 48 images and the accuracy of prediction is only 83.33%. Hence, more cases should be analyzed in order to confirm this as a potential technology for

prediction of kidney abnormalities at early stage in diabetic subjects. Therefore, we conclude that further studies with more images are mandatory to understand the efficacy of iris images for the prediction of kidney ailments. Moreover in the future, advanced deep learning algorithms can be implemented using a large dataset of iris images to improve the accuracy of prediction.

6. References

Asuntha, A., Siddartha, M., Udhaykumar, K., & Srinivasan, A. (2019). Identification of diabetics mellitus using Iridology. *International Journal of Research in Pharmaceutical Sciences*, *10*(3), 1821-1823. DOI: https://doi.org/10.26452/ijrps.v10i3.1325

Ayda, Y. R., Mooventhan, A., Vinothkumar, M. H., Kayelarasi, C. A., Vijaykanth, S., & Manavalan, N. (2021). Comparative study on iris manifestations between COVID-19 severe cases and non-COVID individuals. *Journal of Complementary and Alternative Medical Research*, *14*(1), 53-60. DOI: 10.9734/jocamr/2021/v14i130238

Amerifar, S., Targhi, A. T., & Dehshibi, M. M. (2015, October). Iris the picture of health: Towards medical diagnosis of diseases based on iris pattern. In *2015 Tenth IEEE. International Conference on Digital Information Management (ICDIM)* (pp. 120-123). IEEE. DOI:10.1109/ICDIM.2015.7381861

Bansal, A., Agarwal, R., & Sharma, R. K. (2015). Determining diabetes using iris recognition system. *International journal of diabetes in developing countries*, *35*(4), 432-438. DOI: 10.1007/s13410-015-0296-1

Chaskar, U. M., & Sutaone, M. S. (2012). Learning to predict diabetes from iris image analysis. *International Journal of Biomedical Engineering and Technology*, *9*(1), 88-99. DOI: 10.1504/IJBET.2012.047373

Hiremath, B., Vajrala, N., Balakrishnan, R., Yeshwanth, N., & Jayantha, B. S. (2018, May). Identification of efficient features for detection of diabetes through iris patterns. In *2018 3rd IEEE International Conference on Recent Trends in Electronics, Information & Communication Technology, (RTEICT)* (pp. 2258-2263). IEEE. DOI: 10.1109/RTEICT42901.2018.9012374

Hussein, S. E., Hassan, O. A., & Granat, M. H. (2013). Assessment of the potential iridology for diagnosing kidney disease using wavelet analysis and neural networks. *Biomedical Signal Processing and Control*, *8*(6), 534-541. DOI: 10.1016/j.bspc.2013.04.006

Jensen, B. (2012). Iridology simplified. Oxford , UK: Book Publishing Company.

Jogi, S. P., & Sharma, B. B. (2014, November). Methodology of iris image analysis for clinical diagnosis. In *2014 International Conference on Medical Imaging, m-Health and Emerging Communication Systems* (MedCom) (pp. 235-240). IEEE. DOI:10.1109/MEDCOM.2014.7006010

Othman, Z., & Prabuwono, A. S. (2010, November). Preliminary study on iris recognition system: Tissues of body organs in iridology. In *2010 IEEE EMBS Conference on Biomedical Engineering and Sciences (IECBES)* (pp. 115-119). IEEE. DOI:10.1109/IECBES.2010.5742211

Padmasini, N., Umamaheswari, R., Kalpana, R., & Sikkandar, M. Y. (2020). Comparative study of iris and retinal images for early detection of diabetic mellitus. *Journal of Medical Imaging and Health Informatics, 10*(2), 316-325. DOI: https://doi.org/10.1166/jmihi.2020.2973

Prayitno, A., Wibawa, A. D., & Purnomo, M. H. (2016, October). Early detection study of Kidney Organ Complication caused by Diabetes Mellitus using iris image color constancy. In *2016 International Conference on Information & Communication Technology and Systems (ICTS)* (pp. 146-149). IEEE. DOI: 10.3390/sym12122066

Samant, P., & Agarwal, R. (2018). Machine learning techniques for medical diagnosis of diabetes using iris images. *Computer methods and programs in biomedicine*, *157*, 121-128.

Shampine, L. F., & Reichelt, M. W. (1997). The matlab ode suite. SIAM journal on scientific computing, 18(1), 1-22.

Wibawa, A. D., & Purnomo, M. H. (2006, December). Early detection on the condition of pancreas organ as the cause of diabetes mellitus by real time iris image processing. In *APCCAS 2006-2006. IEEE Asia Pacific Conference on Circuits and Systems* (pp. 1008-1010). IEEEDOI:10.1109/APCCAS.2006.342258